PERFORMANCE OF NOVEL PIEZO-ACTIVE α–β COMPOSITES BASED ON RELAXOR-FERROELECTRIC SINGLE CRYSTALS

V.Yu. Topolov,[1] C.R. Bowen,[2] P. Bisegna,[3] and A.V. Krivoruchko[1]
[1] Department of Physics, Southern Federal University,
5 Zorge Street, 344090 Rostov-on-Don, Russia
[2] Materials Research Centre, Department of Mechanical Engineering,
University of Bath, Bath BA2 7AY, UK
[3] Department of Civil Engineering, University of Rome "Tor Vergata",
00133 Rome, Italy
vutopolov@sfedu.ru

SUMMARY

This work simulates the electromechanical properties and related parameters of $0.67Pb(Mg_{1/3}Nb_{2/3})O_3$–$0.33PbTiO_3$ single crystal / polymer composites with 0–3, 1–3 and 2–2 connectivities. Advantages in performance are related to the presence of the highly piezo-active component. Comparison of results for 0–3 connectivity is made.

Keywords: piezo-active composite; connectivity; electromechanical properties; relaxor-ferroelectric; polymer

INTRODUCTION

Piezo-active composites are an important group of modern smart materials that show a variety of important electromechanical properties and have a remarkable ability to convert mechanical energy and vice versa. These materials are studied and developed in order to improve their performance for sensor, actuator, transducer, hydrophone, and other piezotechnical applications [1–3]. The application of single crystals (SCs) of relaxor-ferroelectric $(1 - x)Pb(Mg_{1/3}Nb_{2/3})O_3 - xPbTiO_3$ (PMN–*x*PT) and $(1 - x)Pb(Zn_{1/3}Nb_{2/3})O_3 - yPbTiO_3$ (PZN–*y*PT) solid solutions as highly effective components of novel piezo-active composites has been proposed in recent experimental work [4–7]. The aforementioned SCs with so-called engineered domain structures and compositions near the morphotropic phase boundary [8–13] are of great interest due to their excellent electromechanical properties (see, e.g., data in Table 1), compared to those of conventional piezoelectric ceramics [3, 14]. Recent results on the SC / polymer composites with 2–2 [15, 16] and 1–3 [17] connectivities suggest that the polarisation orientation effect plays the important role in forming the anisotropic electromechanical properties and the hydrostatic piezoelectric response. Examples of combination of the electromechanical properties in 2–2 SC / polymer composites [16] show that the PMN–*x*PT and PZN–*y*PT SCs promote high piezoelectric sensitivity, activity and considerable hydrostatic piezoelectric response. In the present paper we discuss features of the effective electromechanical properties and high performance of the α–β SC / polymer

Table 1. Room-temperature piezoelectric coefficients d_{ij} (in pC / N) and dielectric permittivities $\varepsilon_{pp}^{\sigma}$ of PMN–*x*PT and PZN–*y*PT SCs with engineered domain structures

	x = 0.28 [10]	x = 0.30 [11]	x = 0.33 [11, 12]	y = 0.045 [13]	y = 0.07 [13]	y = 0.08 [13]
d_{31}	-1283	-921	-1330	-970	-1204	-1455
d_{33}	2365	1981	2820	2000	2455	2890
d_{15}	132	190	146	140	176	159
$\varepsilon_{11}^{\sigma} / \varepsilon_0$	1950	3600	1600	3100	3000	2900
$\varepsilon_{33}^{\sigma} / \varepsilon_0$	6833	7800	8200	5200	5622	7700

composites with the regular arrangement of the SC component. For comparison we consider the composites that are characterised by one of the following connectivities: 2–2, 1–3 or 0–3 (Fig. 1). Interfaces separating the SC and polymer components are planar and continuous (Figs. 1, a and b) in composites with 2–2 and 1–3 connectivities.

MODELLING OF EFFECTIVE ELECTROMECHANICAL PROPERTIES

Our modeling is concerned with composite structures with aligned crystallographic axes in the SC layers (rods, inclusions). In the case of 1–3 connectivity a square arrangement of the SC rods in the (X_1OX_2) plane (Fig. 1, b) is assumed. In the case of 0–3 connectivity it is assumed that centres of symmetry of the SC inclusions (Fig. 1, c) occupy sites of a simple tetragonal lattice with unit-cell vectors parallel to the OX_j axes.

The full set of effective electromechanical constants is determined using the matrix method [3, 15–17] (2–2 and 1–3 connectivities), the effective field method [3, 18] (0–3 connectivity) and finite element method (FEM) [17, 18] (0–3 connectivity). For the 2–2 and 1–3 composites we evaluate elastic compliances s_{ab}^{*E} (measured at electric field E = const), piezoelectric coefficients d_{ij}^{*} and dielectric permittivities $\varepsilon_{pp}^{*\sigma}$ (measured at mechanical stress σ = const) which depend on the volume fraction m of SC. For the 0–3 composite elastic moduli c_{ab}^{*E} (measured at electric field E = const), piezoelectric coefficients e_{ij}^{*} and dielectric permittivities $\varepsilon_{pp}^{*\xi}$ (measured at mechanical strain ξ = const) depend on the volume fraction m and the aspect ratio of the spheroidal inclusion $\rho = a_1 / a_3$. The averaging procedures [3, 15–18] are implemented in a long-wave approximation that is valid when a wavelength of an external acoustic field is much longer than the thickness of the separate layer (rod, inclusion) in the composite sample.

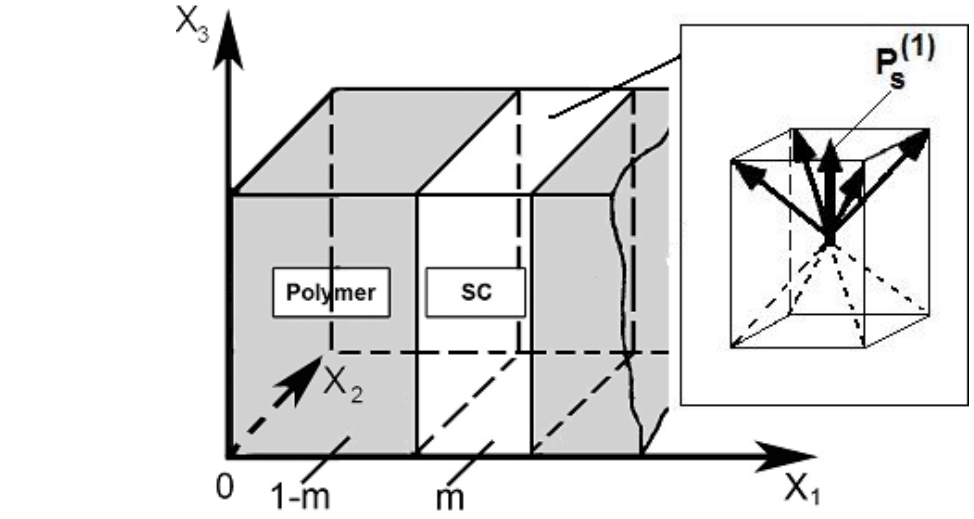

a

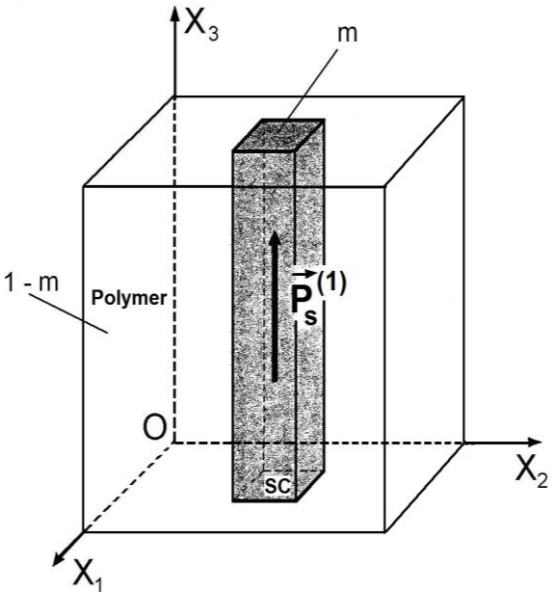

b

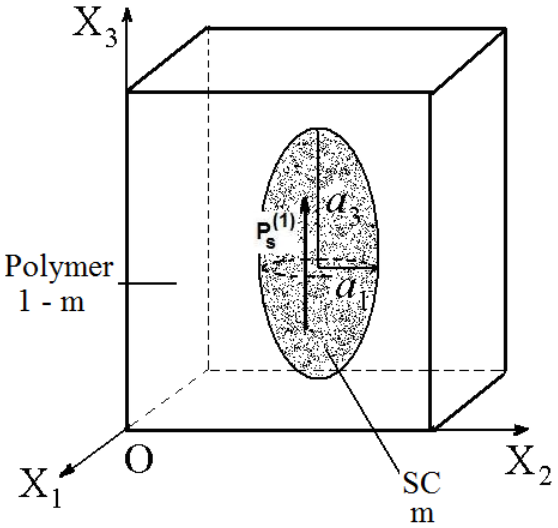

c

Fig. 1. Schematic diagrams of the SC / polymer composites with 2–2 (a), 1–3 (b) and 0–3 (c) connectivities. $\boldsymbol{P}_s^{(1)}$ is the spontaneous polarisation vector of SC, a_1 and a_3 are semiaxes of the spheroidal inclusion. m and $1 - m$ are volume fractions of SC and polymer, respectively. In inset of figure a, the arrangement of domains in the poled SC layer is schematically shown.

RESULTS AND DISCUSSION

In this section we consider examples of volume-fraction behaviour of effective parameters of the α–β SC / polymer composites based on PMN–0.33PT. This composition is located very close to the morphotropic phase boundary [8] and favours the very high piezoelectric activity of SC samples with engineered domain structure [12] at room temperature.

2–2 and 1–3 Composites

The role of relaxor-ferroelectric SC as a component in the 1–3-type composites was analysed and their electromechanical properties were discussed [19] to demonstrate the ranges in which effective composite parameters are most sensitive to material properties and composite architecture, with particular emphasis on where their maximum values are attained. Contrary to examples from work [19], now we consider the 1–3 and 2–2 composites with two piezo-active components. It is assumed that the matrix is made of 75 / 25 mol. % copolymer of vinylidene fluoride and trifluoroethylene (P(VDF)–TrFE). This polymer component is characterised by the piezoelectric coefficients with sgn $e_{3j}^{(2)}$ = –sgn $e_{3j}^{(1)}$ and sgn $d_{3j}^{(2)}$ = –sgn $d_{3j}^{(1)}$ [20] (j = 1 and 3, superscripts "(1)" and "(2)" are related to SC and polymer, respectively), whereas the higher piezoelectric activity of the composite would take place under conditions sgn $e_{3j}^{(2)}$ = sgn $e_{3j}^{(1)}$ and sgn $d_{3j}^{(2)}$ = sgn $d_{3j}^{(1)}$. To increase the piezoelectric activity of the composite, we assume that the SC and polymer components are poled in opposite directions, i.e., the SC component is poled parallel to the OX_3 axis (see Figs. 1, a, b) and the polymer matrix is poled antiparallel to the OX_3 axis. Such a variance of poling is possible due to the considerable difference [11, 21] between the coercive fields of SC and polymer.

We consider volume-fraction dependences of the following effective parameters of the studied composites: longitudinal piezoelectric coefficient d_{33}^*, electromechanical coupling factor $k_{33}^* = d_{33}^* / (\varepsilon_{33}^{*\sigma} s_{33}^{*E})^{1/2}$ and their hydrostatic analogs, $d_h^* = d_{33}^* + d_{32}^* + d_{31}^*$ and $k_h^* = d_h^* / (\varepsilon_{33}^{*\sigma} s_h^{*E})^{1/2}$, where $s_h^{*E} = \sum_{a=1}^{3} \sum_{b=1}^{3} s_{ab}^{*E}$ is a hydrostatic elastic compliance. Results of our calculations based on the matrix method are shown in Fig. 2. It is seen that changes in structure of the composite (cf. Figs. 2, a and 2, b) do not result in considerable changes in the aforementioned effective parameters. This may be the result of an electromechanical interaction between the highly piezo-active SC component and the polymer component that exhibits low piezoelectric activity, but a large piezoelectric anisotropy. Values of d_h^* near the maximum points (see curves 2 in Figs. 2, a, c) are more than those evaluated for the 2–2 parallel-connected PZT-type ceramic / polymer composite [22]. According to data from work [22], $\max d_h^* \approx 60$ pC / N for the ceramic-based composite. The considerable $\max d_h^*$ values in Fig. 2, a can be explained by the presence of the SC component with the piezoelectric coefficients $d_{3j}^{(1)}$ [11, 12] being 4–5 times more than those of the PZT-type ceramic component [14]. It should be added for comparison that the largest d_h^* value (274 pC / N at m = 0.509) has been found [19] for the 1–3 SC / piezo-passive polymer composite with the same PMN–0.33PT composition in the rods. Earlier results of evaluations of the effective electromechanical properties on the basis of the matrix method [3, 15–17] have been compared to results determined using analytical expressions [22] for 2–2 ceramic / polymer composites with the parallel connection of layers. Effective parameters of the 1–3 SC / polymer composite have been determined on the basis of the same matrix method and FEM [17]. Comparison of the volume-fraction dependences of a series of effective parameters calculated using the matrix approach (2–2 and 1–3 connectivities), analytical expressions (2–2 connectivity) and FEM (1–3 connectivity) enables us to conclude the good correlation between these dependences in the wide volume-fraction

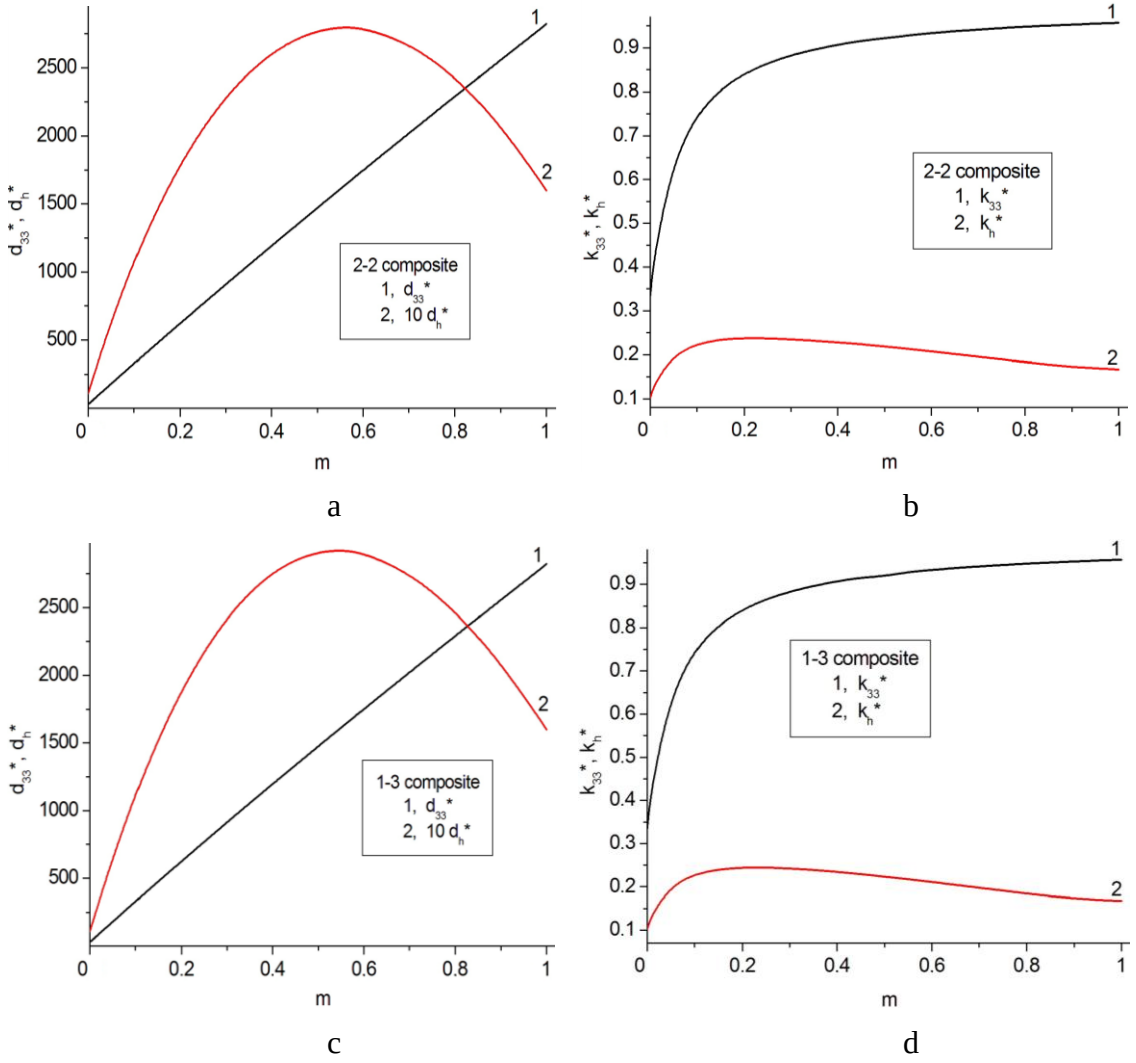

Fig. 2. Volume-fraction dependences of effective parameters calculated for the PMN–0.33PT SC / P(VDF) –TrFE composites with 2–2 (a and b) and 1–3 (c and d) connectivities: piezoelectric coefficients d_{33}^* and d_h^* (a, c, in pC / N) and electromechanical coupling factors k_{33}^* and k_h^* (b, d).

range. Our results indicate potential advantages of the studied 2–2 and 1–3 composites (see data in Fig. 2 and recent papers [15–17, 19]) in actuator, transducer and other piezotechnical applications.

0–3 Composites

In contrast to the 2–2 and 1–3 composites (Figs. 1, a and b), the 0–3 composite represents a system of isolated inclusions distributed in the continuous matrix (Fig. 1, c). The isolated piezo-active inclusions considerably affect the effective parameters of the 0–3 composite as compared to the similar parameters of the 1–3 composite with the same components [18]. To the best of our knowledge, no comparison of the effective parameters calculated using the effective field method and FEM was made in earlier

studies on the 0–3 piezo-active composite with spheroidal inclusions. In this section we consider examples of the piezoelectric response of the 0–3 PMN–0.33PT SC / polymer composite. Its effective electromechanical constants c_{ab}^{*E}, e_{ij}^{*} and $\varepsilon_{pp}^{*\xi}$ are calculated using either the effective field method or FEM. The piezoelectric coefficients d_{ij}^{*}, g_{ij}^{*} and h_{ij}^{*} are evaluated from c_{ab}^{*E}, e_{ij}^{*} and $\varepsilon_{pp}^{*\xi}$ in accordance with formulae [23] for a piezoelectric medium. Experimental elastic and dielectric constants of polymer components are taken from work [24].

An important advantage of the effective field method [3] is that it takes into account the electromechanical interaction between the piezo-active inclusions (in our case aligned SC inclusions) and related coupled effects. An effective field, caused by an external field applied to the composite sample and by interactions "inclusion – matrix" and "inclusions – inclusions" therein, plays the role of an average field approximated by constrained strain and electric fields [3, 18] in a heterogeneous piezo-active medium. In present work the COMSOL package [25] is applied to obtain the volume fraction dependence of the effective electromechanical properties of the 0–3 composite based on SC with high piezoelectric activity. In particular, a unit cell, containing the spheroidal inclusion (see Fig. 1, c) with radius adjusted to yield the appropriate volume fraction *m*, is discretised using 50,000 to 200,000 tetrahedral elements, depending on the aspect ratio ρ of the spheroidal inclusion. The unknown displacement and electric-potential fields are interpolated using linear Lagrangian shape functions, leading to a problem with 30,000 to 150,000 degrees of freedom. Periodic boundary conditions are enforced on the boundary of the unit cell, and the matrix of effective constants of the composite is computed column-wise, performing calculations for diverse average strain and electric fields imposed to the structure. After solving the equilibrium problem, the effective material constants are computed, by averaging the resulting local stress and electric-displacement fields over the unit cell.

Fig. 3 shows the effect of the volume fraction *m* and the aspect ratio ρ on the longitudinal piezoelectric activity (d_{33}^{*}) and sensitivity ($g_{33}^{*} = d_{33}^{*}/\varepsilon_{33}^{*\sigma}$) of the 0–3 composite with spheroidal SC inclusions. The prolate shape of the SC inclusion with the lower ρ value promotes the higher piezoelectric activity of the composite at *m* = const (Fig. 3, a). This shape is also favourable to attain the considerable piezoelectric sensitivity (see curves 1 and 2 in Fig. 3, b) due to the relative large piezoelectric coefficient d_{33}^{*} at relatively low dielectric permittivity $\varepsilon_{33}^{*\sigma}$. It should be noted that at ρ = 0.1 the ratio of $\max g_{33}^{*}/g_{33}^{(1)} = 5.2$ is attained. We mention for comparison that the 1–3 PMN–0.33PT SC / araldite composite with the parallelepiped-shaped rods (see Fig. 1, b) is characterised by $\max g_{33}^{*}/g_{33}^{(1)} = 12.8$ [19]. Thus, changes in connectivity and forming the isolated SC inclusions would lead in essential decreasing the longitudinal piezoelectric sensitivity of the composite.

Comparing results on the effective piezoelectric coefficients from Table 2, we see a certain correlation between volume-fraction dependences calculated using the effective field method and FEM. We note that the piezoelectric coefficients listed in Table 2 are not calculated directly from the averaging procedure. In both methods this procedure enables us to evaluate e_{ij}^{*}, and the remaining piezoelectric coefficients are determined

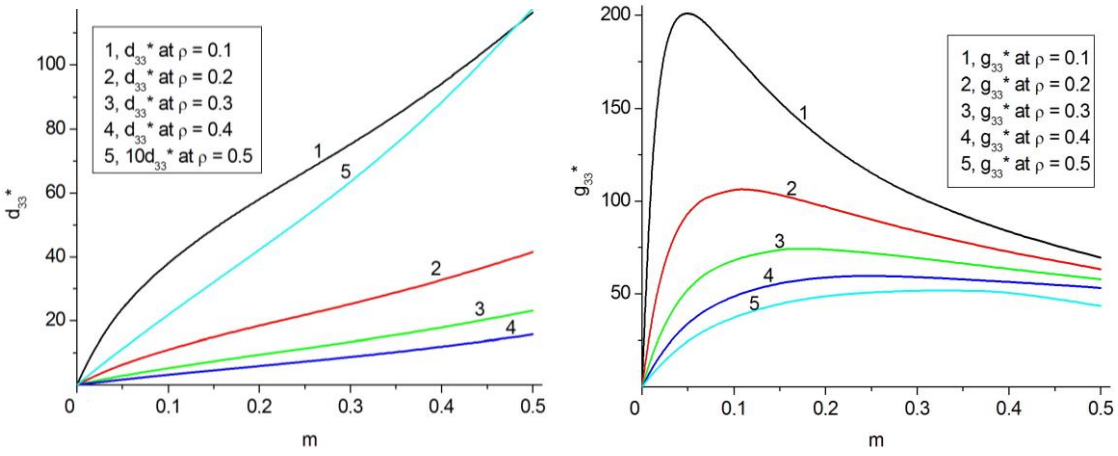

a b

Fig. 3. Volume-fraction dependences of effective piezoelectric coefficients calculated for the 0–3 PMN–0.33PT SC / araldite composite be means of the effective field method: a, d_{33}^* (in pC / N) and b, g_{33}^* (in mV·m / N).

using the full set of the effective constants averaged. Good agreement between the effective parameters shown in Table 2 is attained at ρ > 0.2, i.e., when a transition from the highly prolate inclusion shape to the prolate one takes place. Our evaluations suggest that the largest d_{33}^* value listed in Table 2 remains about 70 times less than the piezoelectric coefficient $d_{33}^{(1)}$ of SC, and the ratio $e_{3j}^* / e_{3j}^{(1)} << 1$ also holds at the *m* and ρ values from Table 2. At the same time, smaller differences are attained for the effective piezoelectric coefficients $g_{33}^* = d_{33}^* / \varepsilon_{33}^{*\sigma}$ or $h_{33}^* = e_{33}^* / \varepsilon_{33}^{*\xi}$ (see Table 2). In the wide *m* ranges g_{33}^* and h_{33}^* become comparable to the similar piezoelectric coefficients $g_{33}^{(1)}$ and $h_{33}^{(1)}$ of SC, and agreement between the corresponding calculated values is attained.

An additional reason for the difference between d_{3j}^* calculated using different methods may be concerned with a relatively small ratio of the elastic constants of the SC and polymer and the large ratio of their dielectric constants. According to our evaluations based on experimental constants of components [12, 24], ratios $c_{11}^{(1),E} / c_{11}^{(2)} = 14.7$ and $c_{33}^{(1),E} / c_{11}^{(2)} = 13.2$ are order-of-magnitude less than $\varepsilon_{33}^{(1),\xi} / \varepsilon_{33}^{(2)} = 170$. This circumstance undoubtedly affects a re-distribution of internal electric and mechanical fields in the studied composite and leads us to believe that the effective field method could be applied with some restrictions for 0–3 connectivity. We note, that in recent paper [18] on the 1–3 $PbTiO_3$ ceramic / polymer composite, good agreement between the parameters calculated by the same methods is attained when ratios $c_{11}^{(1),E} / c_{11}^{(2)} \approx 24$, $c_{33}^{(1),E} / c_{11}^{(2)} \approx 23$ and $\varepsilon_{33}^{(1),\xi} / \varepsilon_{33}^{(2)} \approx 31 \ldots 37$ hold. Table 3 suggests that in the presence of the prolate SC inclusions in the polyurethane matrix ($c_{11}^{(1),E} / c_{11}^{(2)} = 26.0$, $c_{33}^{(1),E} / c_{11}^{(2)} = 23.3$ and $\varepsilon_{33}^{(1),\xi} / \varepsilon_{33}^{(2)} = 194$) good agreement is observed for cases of the piezoelectric coefficients d_{33}^* and g_{33}^* in the wide *m* range.

Table 2. Calculated effective piezoelectric coefficients d_{3j}^{*} (in pC / N), g_{33}^{*} (in mV·m / N) and h_{33}^{*} (in 10^9 V / m) of the 0–3 PMN–0.33PT SC / araldite composite

	d_{33}^{*} (effective field method)				d_{33}^{*} (FEM)			
m	ρ = 0.2	ρ = 0.3	ρ = 0.4	ρ = 0.5	ρ = 0.2	ρ = 0.3	ρ = 0.4	ρ = 0.5
0.01	1.46	0.624	0.353	0.234	1.26	0.633	0.394	0.271
0.03	4.07	1.79	1.03	0.690	2.60	1.56	1.04	0.741
0.05	6.35	2.86	1.67	1.13	3.44	2.24	1.57	1.16
0.10	11.1	5.26	3.17	2.19	4.74	3.49	2.64	2.07
0.20	18.5	9.41	5.93	4.22	6.57	5.19	4.26	3.60
0.30	25.2	13.4	8.68	6.32	8.66	6.92	5.85	5.14
0.40	32.4	17.8	11.8	8.73	11.9	9.56	8.21	7.38
0.50	41.5	23.2	15.7	11.8	21.4	17.7	15.5	14.3
	d_{31}^{*} (effective field method)				d_{31}^{*} (FEM)			
m	ρ = 0.2	ρ = 0.3	ρ = 0.4	ρ = 0.5	ρ = 0.2	ρ = 0.3	ρ = 0.4	ρ = 0.5
0.01	-0.562	-0.249	-0.147	-0.102	-0.490	-0.250	-0.160	-0.110
0.03	-1.574	-0.717	-0.429	-0.300	-1.04	-0.630	-0.430	-0.320
0.05	-2.47	-1.15	-0.700	-0.494	-1.40	-0.930	-0.660	-0.500
0.10	-4.37	-2.15	-1.34	-0.961	-1.99	-1.49	-1.14	-0.920
0.20	-7.50	-3.93	-2.55	-1.88	-2.84	-2.29	-1.91	-1.64
0.30	-10.5	-5.70	-3.80	-2.84	-3.77	-3.09	-2.66	-2.37
0.40	-13.8	-7.71	-5.24	-3.96	-5.16	-4.25	-3.72	-3.38
0.50	-18.1	-10.3	-7.06	-5.39	-8.80	-7.42	-6.59	-6.12
	g_{33}^{*} (effective field method)				g_{33}^{*} (FEM)			
m	ρ = 0.2	ρ = 0.3	ρ = 0.4	ρ = 0.5	ρ = 0.2	ρ = 0.3	ρ = 0.4	ρ = 0.5
0.01	35.2	16.0	9.28	6.26	31.4	16.3	10.4	7.25
0.03	74.8	38.3	23.7	16.6	55.7	35.2	24.4	18.0
0.05	93.5	52.4	34.1	24.6	66.0	45.8	33.6	25.9
0.10	106	69.1	49.3	37.8	73.6	58.1	46.6	38.4
0.20	97.0	74.0	59.0	49.0	72.5	62.6	55.0	49.2
0.30	83.4	69.4	59.7	51.7	68.5	61.2	56.2	52.5
0.40	72.2	63.4	59.1	51.2	64.7	59.5	56.2	54.0
0.50	63.3	57.7	53.2	49.5	65.0	62.5	60.7	59.7
	h_{33}^{*} (effective field method)				h_{33}^{*} (FEM)			
m	ρ = 0.2	ρ = 0.3	ρ = 0.4	ρ = 0.5	ρ = 0.2	ρ = 0.3	ρ = 0.4	ρ = 0.5
0.01	0.165	0.0715	0.0398	0.0257	0.146	0.0732	0.0451	0.0304
0.03	0.392	0.186	0.109	0.0719	0.286	0.170	0.112	0.0796
0.05	0.544	0.275	0.166	0.113	0.371	0.238	0.165	0.121
0.10	0.778	0.435	0.280	0.198	0.505	0.361	0.267	0.207
0.20	1.04	0.641	0.444	0.331	0.689	0.530	0.425	0.352
0.30	1.22	0.800	0.578	0.446	0.865	0.686	0.573	0.498
0.40	1.40	0.955	0.711	0.562	1.08	0.884	0.769	0.696
0.50	1.59	1.13	0.861	0.695	1.54	1.38	1.28	1.22

Table 3. Calculated effective piezoelectric coefficients d_{3j}^* (in pC / N) and g_{33}^* (in mV·m / N) of the 0–3 PMN–0.33PT SC / polyurethane composite

	d_{33}^* (effective field method)		d_{33}^* (FEM)		g_{33}^* (effective field method)		g_{33}^* (FEM)	
m	ρ = 0.3	ρ = 0.5	ρ = 0.3	ρ = 0.5	ρ = 0.3	ρ = 0.5	ρ = 0.3	ρ = 0.5
0.01	0.592	0.215	0.614	0.254	17.3	6.57	18.1	7.75
0.03	1.69	0.633	1.50	0.689	41.2	17.3	38.7	19.1
0.05	2.69	1.03	2.14	1.08	56.0	25.6	50.0	27.4
0.10	4.88	1.99	3.29	1.91	73.0	39.2	62.6	40.5
0.20	8.57	3.80	4.79	3.29	76.9	50.4	65.9	51.4
0.30	12.1	5.66	6.29	4.66	71.3	52.7	63.5	54.3
0.40	15.9	7.77	8.60	6.63	64.7	52.1	61.1	55.5
0.50	20.7	10.4	15.9	12.9	58.6	50.1	63.9	61.4

CONCLUSION

In the present paper modelling and property predictions have been carried out within the framework of the models of the α–β SC / polymer composites with structures shown in Fig. 1. The large values of the piezoelectric coefficients $g_{33}^* \sim 10^2$ mV·m / N and $d_h^* \sim 10^2$ pC / N and electromechanical coupling factor $0.5 < k_{33}^* < 0.95$ are attainable in the 2–2 and 1–3 composites due to their microgeometry and high piezoelectric activity of SC ($d_{3j}^{(1)} \sim 10^3$ pC / N). Comparison of the piezoelectric coefficients calculated by the effective field method and FEM has been carried out for the 0–3 composite based on PMN–0.33PT SC, and reasons for differences between the calculated constants have been discussed. Results on the electromechanical properties studied in this work can be taken into consideration at prediction of the effective parameters and further applications of the advanced composites based on relaxor-ferroelectric SCs.

ACKNOWLEDGEMENTS

The authors would like to thank Prof. Dr. R. Stevens (University of Bath, UK), Prof. Dr. A.V. Turik and Prof. Dr. A.E. Panich (Southern Federal University, Russia), and Dr. M. Kamlah (Karlsruhe Research Centre, Germany) for their interest in the research problems. This work was partially supported by the administration of the Southern Federal University (Project No. 11.01.09f on basic research).

References

1. E.K. Akdogan, M. Allahverdi, A. Safari, IEEE Trans. Ultrason., Ferroelec., a. Freq. Contr. **52**, 746–775 (2005).
2. H.L.W. Chan, I.L. Guy, Key Engin. Mater. **92–93**, 275–300 (1994).
3. V.Yu. Topolov, C.R. Bowen, *Electromechanical properties in composites based on ferroelectrics* (London: Springer, 2009).

4. T. Ritter, X. Geng, K.K. Shung et al., IEEE Trans. Ultrason., Ferroelec., a. Freq. Contr. **47**, 792–800 (2000).

5. K.C. Cheng, H.L.W. Chan, C.L. Choy et al., IEEE Trans. Ultrason., Ferroelec., a. Freq. Contr. **50**, 1177–1183 (2003).

6. K. Ren, Y. Liu, X. Geng et al., IEEE Trans. Ultrason., Ferroelec., a. Freq. Contr. **53**, 631–638 (2006).

7. F. Wang, C. He, Y. Tang et al., Mater. Chem. Phys. **105**, 273–277 (2007).

8. B. Noheda, Curr. Opinion Solid St. Mater. Sci. **6**, 27–34 (2002).

9. L.E. Cross, in: *Piezoelectricity: Evolutions and future of technology*, Eds. W. Heywang, K. Lubitz, W. Wersing (Berlin, Heidelberg: Springer, 2008), p.131–155.

10. D. Zhou, F. Wang, L. Luo et al., J. Phys. D: Appl. Phys. **41**, 185402–4 p. (2008).

11. H. Cao, V.H. Schmidt, R. Zhang et al., J. Appl. Phys. **96**, 549–554 (2004).

12. R. Zhang, B. Jiang, W. Cao, J. Appl. Phys. **90**, 3471–3475 (2001).

13. R. Zhang, B. Jiang, W. Cao, A. Amin, J. Mater. Sci. Lett. **21**, 1877–1879 (2002).

14. B. Jaffe, W.R. Cook, H. Jaffe H, *Piezoelectric ceramics* (London, New York: Academic Press, 1971).

15. A.V. Krivoruchko, V.Yu. Topolov, J. Phys. D.: Appl. Phys. **40**, P.7113–7120 (2007).

16. V.Yu. Topolov, A.V. Krivoruchko, J. Appl. Phys. **105**, 074105–7 p. (2009).

17. V.Yu. Topolov, A.V. Krivoruchko, P. Bisegna, C.R. Bowen, Ferroelectrics **376**, 140–152 (2008).

18. V.Yu. Topolov, P. Bisegna, A.V. Krivoruchko, J. Phys. D: Appl. Phys. **41**, 035406–8 p. (2008).

19. S.V. Bezus, V.Yu. Topolov, C.R. Bowen, J. Phys. D: Appl. Phys. **39**, 1919–1925 (2006).

20. H. Taunaumang, I.L. Guy, H.L.W. Chan, J. Appl. Phys. **76**, 484–489 (1994).

21. G.M. Sessler, J. Acoust. Soc. Amer. **70**, 1596–1608 (1991).

22. A.A. Grekov, S.O. Kramarov, A.A. Kuprienko, Ferroelectrics **76**, 43–48 (1987).

23. T. Ikeda, *Fundamentals of piezoelectricity* (Oxford, New York, Toronto: Oxford University Press, 1990).

24. S.V. Glushanin, V.Yu. Topolov, A.V. Krivoruchko, Materials Chem. a. Phys. **97**, 357–364 (2006).

25. COMSOL, Inc. 2007 COMSOL Multiphysics™ User's Guide (version 3.3a), http://www.comsol.com/